INT. J. CONTROL, 1992, VOL. 56, NO. 5, 1211–1241

Subspace model identification
Part 2. Analysis of the elementary output-error state-space model identification algorithm

MICHEL VERHAEGEN† and PATRICK DEWILDE†

The elementary MOESP algorithm presented in the first part of this series of papers is analysed in this paper. This is done in three different ways. First, we study the asymptotic properties of the estimated state-space model when only considering zero-mean white noise perturbations on the output sequence. It is shown that, in this case, the MOESP1 implementation yields asymptotically unbiased estimates. An important constraint to this result is that the underlying system must have a finite impulse response and subsequently the size of the Hankel matrices, constructed from the input and output data at the beginning of the computations, depends on the number of non-zero Markov parameters. This analysis, however, leads to a second implementation of the elementary MOESP scheme, namely MOESP2. The latter implementation has the same asymptotic properties without the finite impulse response constraint. Secondly, we compare the MOESP2 algorithm with a classical state space model identification scheme. The latter scheme, referred to as the CLASSIC algorithm, is based on the Ho and Kalman realization scheme and estimated Markov parameters. The comparison is done by a sensitivity study, where the effect is studied of the errors on the data on the calculated column space of the shift-invariant subspace. This study demonstrates that the elementary MOESP2 scheme is more robust with respect to the errors considered than the CLASSIC algorithm. In the third part, the model reduction capabilities of the elementary MOESP schemes are analysed when the observations are error-free. We demonstrate in which sense the reduced order model is optimal when acquired with the MOESP schemes. The optimality is expressed by the difference between the 2-norm of the errors on the state (or output) sequence of the reduced-order model and the 2-norm of the matrix containing the rejected singular values being as small as possible. The insights obtained in these three parts are evaluated in a simulation study, and validated in this paper. They lead to the assertion that the MOESP2 implementation allows identification of a compact, low-dimensional, state-space model accurately describing the input–output behaviour of the system to be identified, while making use of 'perturbed' input–output data. This can be done efficiently.

1. Introduction

In this paper, we study the identification and model reduction capabilities of the elementary MOESP algorithm presented in the first part of this series.

The identification problem analysed is a simplified version of the collective problem stated by Verhaegen and Dewilde (1992). With the help of Fig. 1, we define this problem as follows.

A simple identification problem: *given* a finite and exactly known input sequence u_k and its corresponding output sequence z_k, the latter se-

Received 30 April 1991. Revised 30 September 1991 and 16 December 1991.

† Department of Electrical Engineering, Delft University of Technology, P.O. Box 5031, NL-2600 GA Delft, The Netherlands.

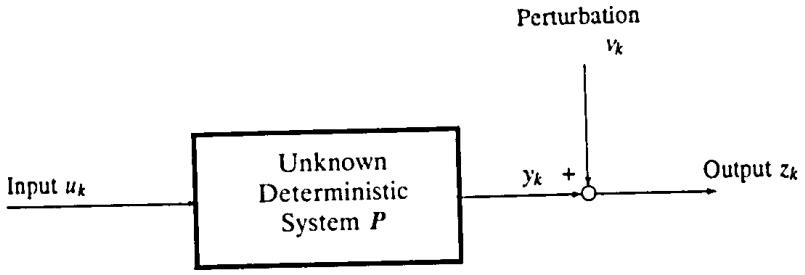

Figure 1. Block schematic view of a simple system identification set-up.

quence is *assumed* to be perturbed by an unknown zero-mean white noise sequence v_k, statistically independent from the input sequence. Then, the task is to *approximate* a shift-invariant or structured subspace of spaces defined by the input–output data. This subspace should determine a state-space model that represents the input–output behaviour of the linear time-invariant finite-dimensional system in the block $\boldsymbol{P}$ of Fig. 1.

Such a simple identification problem has very limited practical value. However, the insights from this simple framework will be important in analysing more complicated identification problems. In this way, we may compare the results obtained in this paper with the insights that have been gathered from studies of the simple linear least-squares problem. These insights have served as the cornerstone in the analysis of other identification problems where nonlinear least-squares problems occur (Ljung 1987 and Söderström and Stoica 1989).

When the system has multiple inputs and multiple outputs (an MIMO system), the basic identification problem can be solved by the scheme recently proposed by Moonen and Vandewalle (1990). However, algorithmically this scheme is more complicated since it requires the use of the generalized SVD (Golub and Van Loan 1989). In the elementary MOESP scheme we have seen that only an ordinary SVD is required. Therefore, we observe that the algorithm of Moonen and Vandewalle (1990) will solve the basic problem in a complicated way. In addition, because the underlying principles that give rise to both implementations are different, we will not pursue an analysis of the relationship between both algorithms any further in this paper.

Another existing solution, mentioned by Verhaegen and Dewilde (1992), is borrowed from the realization theory developed by Ho and Kalman (1966). In an identification framework, the same algorithm can be used, now based on estimated Markov parameters. The latter quantities can be estimated (see, e.g. Verhaegen 1991 b) from the input–output data by solving a least-squares problem. Experience with this approach has demonstrated that it is very sensitive to errors on the data, especially when relying on a restricted number of Markov parameters (Verhaegen 1991 b).

The data used by the elementary MOESP algorithm consists, apart from the input–output data, of a restricted number of Markov parameters. Hence, this scheme is related to the classical solution based on Markov parameters only. In order to reveal the usefulness of both solutions, a detailed sensitivity analysis is performed in this paper.

The organization of this paper is a continuation of that established in Part 1. The notation is compatible with that used in Part 1. For the sake of continuity

we compile the different proofs and propositions at the end of the paper in Appendices A and B, respectively, unless otherwise stated.

In § 2, we investigate the asymptotic unbiasedness of the elementary MOESP1 implementation, simply referred to as the MOESP1 algorithm. This leads to a more favourable implementation, indicated by the MOESP2 algorithm. The classical algorithm based only on estimated Markov parameters and the sensitivity study on the effect of error-affected data on the calculation of the shift-invariant subspace is presented in § 3; § 4 discusses the model reduction capabilities of the elementary MOESP schemes. The obtained insights are verified by means of a series of simulations in § 5. The concluding remarks summing up some useful properties of the elementary MOESP schemes are given in § 6.

2. Performance of the MOESP1 scheme when the system output is contaminated by errors

From the algorithmic summary of the MOESP1 algorithm, given in § 4.3 of Part 1, a number of quantities influence the estimates obtained with this algorithm. In this section, we study the influence of those quantities which are inherent to the identification problem at hand and therefore not within the control of the user. These are:

(*a*) the estimation of the Markov parameters, necessary in the Toeplitz matrix H_i (see its definition in (7)–(8) of Part 1);

(*b*) conditions on the stochastic process v_k in (3) of Part 1 which guarantee an asymptotically unbiased estimate of the state space quadruple.

In this and the following section, we will mark the quantities related to the error-affected output measurement z_j and estimated Markov parameters by a ($\tilde{}$). The estimates of the above problems will be studied in the ergodic statistical framework, outlined in § 2.3 of Part 1.

2.1. *Estimating the Markov parameters*

It is a well-known result in identification theory (e.g., see Chen 1970), that when the underlying system (represented by (1)–(3) of Part 1) is asymptotically stable and v_k is an arbitrary but zero-mean stochastic process statistically independent from the input, the Markov parameters $h_j = CA^{j-1}B$ for $j = 1, 2, \ldots$ and $h_0 = D$ can be estimated by simple least-squares in a statistically consistent manner. In the context of § 2.3 of Part 1, this result is summarized in the following lemma. First we define the *finite impulse response model* representation.

Definition 1: A linear time-invariant and finite-dimensional linear system given by (1)–(2) of Part 1 is representable by a finite impulse response (FIR) model of order κ, if and only if the output of the system to an input sequence $\{u_k\}$ satisfies

$$y_k = \sum_{j=1}^{\kappa-1} CA^{j-1}Bu_{k-j} + Du_k \qquad (1)$$

□

Lemma 1: *Let the system* (1)–(3) *of Part 1 be represented by an FIR model of order* κ. *Furthermore, let* u_k *be a persistently excited input of order* κ, *and let the zero-mean perturbation* v_k *be statistically independent from the input, then:*

$$\lim_{N\to\infty} \frac{1}{N} Z_{\kappa,1,N+\kappa-1} U_{1,\kappa,N}^{\mathrm{T}} \left(\frac{1}{N} U_{1,\kappa,N} U_{1,\kappa,N}^{\mathrm{T}}\right)^{-1} = [CA^{\kappa-2}B \quad \ldots \quad CB \quad D] \tag{2}$$

For a proof of this lemma (in terms of mathematical expectations), we refer to Chen (1970).

In the study of the unbiasedness of the MOESP1 algorithm, we will assume that the conditions of Lemma 1 hold and hence that we know the restricted set of Markov parameters in the matrix H_i of (8) in Part 1 exactly. This allows us to investigate the effect of the errors on the output separately. The above assumption is motivated by the fact that both estimation problems can be solved independently.

The investigation of the effect of error-affected data on the solution of the least-squares problem, denoted by (40) of Part 1, is done in Theorem 1. In the first place, we need a result on the calculation of the invariant subspace of a perturbed positive semidefinite matrix.

2.2. *Some results on the invariant subspaces of a perturbed positive semidefinite matrix*

The analysis given in this section focuses on positive semidefinite matrices which are obtained by multiplication of a rectangular $l.i \times N$ matrix and its transposition, with $l.i \ll N$, of rank n. These dimensions correspond to the indices l, i, n and N introduced in (1)–(2) and (7) of Part 1.

Lemma 2: *Let the matrix* F_N *and its perturbation* $\tilde{F}_N = F_N + V_N \in \mathbb{R}^{l.i\times N}$, *satisfy:*

(1)
$$\lim_{N\to\infty} \frac{1}{N} F_N F_N^{\mathrm{T}} = U_F S_F^2 U_F^{\mathrm{T}} \tag{3}$$

with S_F *an* $n \times n$ *diagonal matrix and* $n < l.i$

(2)
$$\lim_{N\to\infty} \frac{1}{N} F_N V_N^{\mathrm{T}} = 0 \tag{4}$$

(3)
$$\lim_{N\to\infty} \frac{1}{N} V_N V_N^{\mathrm{T}} = \sigma^2 I_{l.i} \tag{5}$$

then,

$$\lim_{N\to\infty} \frac{1}{N} \tilde{F}_N \tilde{F}_N^{\mathrm{T}} = [U_F | U_F^{\perp}] \left[\begin{array}{c|c} S_F^2 + \sigma^2 I_n & 0 \\ \hline 0 & \sigma^2 I_{l.i-n} \end{array}\right] \left[\begin{array}{c} U_F^{\mathrm{T}} \\ \hline (U_F^{\perp})^{\mathrm{T}} \end{array}\right] \tag{6}$$

with $U_F^{\perp}$ *such that*

$$[U_F | U_F^{\perp}] \left[\begin{array}{c} U_F^{\mathrm{T}} \\ \hline (U_F^{\perp})^{\mathrm{T}} \end{array}\right] = I_{l.i}$$

Proof: For the proof, see Appendix A.1. □

The entries of the matrix V_N in the above lemma represent zero-mean white noise errors added to the entries of the 'error-free' matrix F_N.

This lemma leads to the following two corollaries.

Corollary 1: *Let the singular value decomposition of the matrix $\tilde{F}_N$ be given as*

$$\tilde{F}_N = (U_{\tilde{F}_N}(:, 1{:}n)|U_{\tilde{F}_N}(:, n+1{:}li))(S_{\tilde{F}_N})\begin{pmatrix}(V_{\tilde{F}_N}(:, 1{:}n))^{\mathrm{T}}\\(V_{\tilde{F}_N}(:, n+1{:}li))^{\mathrm{T}}\end{pmatrix} \tag{7}$$

with the singular values ordered in ascending order such that $S_{\tilde{F}_N}(j, j) \geq S_{\tilde{F}_N}(j+1, j+1)$ for $j = 1, \ldots, l.i-1$, and let $\mathrm{span}_{\mathrm{col}}$ denote the span of the column space, then,

$$\lim_{N\to\infty} \mathrm{span}_{\mathrm{col}}\, U_{\tilde{F}_N}(:, 1{:}n) = \mathrm{span}_{\mathrm{col}}\, U_F$$

$$\lim_{N\to\infty} \mathrm{span}_{\mathrm{col}}\, U_{\tilde{F}_N}(:, n+1{:}li) = \mathrm{span}_{\mathrm{col}}\, U_F^{\perp}$$

Proof: For the proof, see Appendix A.2. □

Since the individual spectra of $S_F^2 + \sigma^2 I_n$ and $\sigma^2 I_{l.i-n}$ may (will) coincide, the result of Corollary 1 can also be written as

$$\lim_{N\to\infty} U_{\tilde{F}_N}(:, 1{:}n) = \lim_{N\to\infty} U_F M_{1_N} \quad \text{and} \quad \lim_{N\to\infty} U_{\tilde{F}_N}(:, n+1{:}li) = \lim_{N\to\infty} U_F^{\perp} M_{2_N} \tag{8}$$

where $\{M_{1_N} \in \mathbb{R}^{n\times n}\}$ and $\{M_{2_N} \in \mathbb{R}^{(l.i-n)\times(l.i-n)}\}$ are sequences of orthonormal matrices. For example, when considering the left-hand side equality, the equivalence means that there will always exist an orthonormal matrix M_{1_N} and an integer N_1 such that for $N > N_1$, the difference $U_{\tilde{F}_N}(:, 1{:}n) - U_F M_{1_N}$ can be made arbitrary small.

Corollary 2: *Let the definitions in Corollary 1 hold and let the matrices F_N, V_N and $U_N \in \mathbb{R}^{m.i\times N}$ satisfy,*

$$\lim_{N\to\infty} \frac{1}{N} V_N U_N^{\mathrm{T}} = 0; \quad \lim_{N\to\infty} \frac{1}{N} F_N U_N^{\mathrm{T}} \text{ exist and } \mathrm{span}_{\mathrm{col}}\, F_N = \mathrm{span}_{\mathrm{col}}\, U_F$$

and let $\{M_{2_N} \in \mathbb{R}^{(l.i-n)\times(l.i-n)}\}$ be a sequence of orthonormal matrices, then,

$$\lim_{N\to\infty} \frac{1}{N} M_{2_N} S_{\tilde{F}_N}(n+1{:}li, n+1{:}li)(V_{\tilde{F}_N}(:, n+1{:}li))^{\mathrm{T}} U_N^{\mathrm{T}} = 0 \tag{9}$$

Proof: For the proof, see Appendix A.3. □

2.3. *Unbiasedness of the MOESP1 algorithm*

Before stating the main result of this section, we need two other lemmas.

The first lemma comments on the full row rank condition (28) of Part 1 when the output y_k is perturbed by the error v_k.

When the input sequence u_k is ergodic, and hence x_k is also ergodic, then condition (28) of Part 1 can be stated in view of the discussion given after Definition 1 of Part 1 of persistency of excitation as the persistency of excitation (of order 1) of the signal $(u_k^{\mathrm{T}} \ \ldots \ u_{k+i-1}^{\mathrm{T}}|x_k^{\mathrm{T}})^{\mathrm{T}}$. This condition holds when multiplying x_k by a non-singular $n \times n$ transformation matrix T. To see this, denote the following limits:

$$\left.\begin{aligned}
&\lim_{N\to\infty}\frac{1}{N}TX_{1,N}X_{1,N}^{\mathrm{T}}T^{\mathrm{T}} = TP_XT^{\mathrm{T}}\\
&\lim_{N\to\infty}\frac{1}{N}TX_{1,N}U_{1,i,N}^{\mathrm{T}} = TR_{XU} = {}_n\left[\begin{array}{c|c} {}^m TR_{XU_1} & \star \end{array}\right]\\
&\lim_{N\to\infty}\frac{1}{N}U_{1,i,N}U_{1,i,N}^{\mathrm{T}} = R_U = {}^m\left[\begin{array}{c|c} {}^m R_{U_1} & \star \\ \hline \star & \star \end{array}\right]
\end{aligned}\right\} \tag{10}$$

then the persistency of excitation of the signal $(u_k^{\mathrm{T}} \ldots u_{k+i-1}^{\mathrm{T}} | x_k^{\mathrm{T}})^{\mathrm{T}}$ corresponds to:

$$\rho\left(\lim_{N\to\infty}\frac{1}{N}\left[\begin{array}{c} X_{1,N} \\ \hline U_{1,i,N} \end{array}\right][X_{1,N}^{\mathrm{T}} | U_{1,i,N}^{\mathrm{T}}]\right) = \rho\left(\left[\begin{array}{c|c} P_X & R_{XU} \\ \hline R_{XU}^{\mathrm{T}} & R_U \end{array}\right]\right) = m.i + n \tag{11}$$

Hence, for some non-singular transformation matrix T, the matrix

$$\left[\begin{array}{c|c} TP_XT^{\mathrm{T}} & TR_{XU} \\ \hline R_{XU}^{\mathrm{T}}T^{\mathrm{T}} & R_U \end{array}\right]$$

remains positive definite.

Based on this way of interpreting condition (28) in the ergodic signal framework, we have the following lemma.

Lemma 3: *Let the input u_k and state x_k be ergodic signals, such that the conditions in* (10) *and* (11) *hold, let v_j be a zero-mean white noise sequence with variance σ_v^2 and orthogonal to u_k and x_k, and let T_1 be an $n \times n$ invertible matrix and $T_2 \in \mathbb{R}^{n \times l.i}$, then the signal*

$$\left[\begin{array}{c} T_1x_k + T_2\left[\begin{array}{c} v_k \\ \vdots \\ v_{k+i-1} \end{array}\right] \\ \hline u_k \end{array}\right]$$

is persisently excited (of order 1*).*

Proof: For the proof, see Appendix A.4. □

The second lemma evaluates the pseudo-inverse $(U_n^{(1)})\dagger$ used in the calculations of the elementary MOESP1 algorithm when the dimension parameter i satisfies a particular constraint.

Lemma 4: *Let,*

(1) *the plant* **P** *be representable by the state-space model given by* (1)–(2) *in Part* 1 *of order n and an FIR model of order* κ *given by equation* (1) *of this Part*;

(2) $i \geq \kappa$ *and* $i > n$,

(3) *the input* u_k *be such that condition* (28) *of Part* 1 *is satisfied; and*

(4) *the SVD of the matrix* $\Gamma_i X_{1,N}$ *be:*

$$\Gamma_i X_{1,N} = li \begin{bmatrix} n & l.i-n \\ U_n & U_n^{\perp} \end{bmatrix} S \bar{V}^{\mathrm{T}} \tag{12}$$

then,

$$(U_n^{(1)})\dagger (U_n^{\perp})^{(1)} = 0 \quad \textit{and} \quad (U_n^{(1)})\dagger = (U_n^{(1)})^{\mathrm{T}} \tag{13}$$

where $(.)\dagger$ *and* $(.)^{(1)}$ *respectively denote a left pseudo-inverse and the submatrix composed of the first* $(i-1)l$ *rows.*

Proof: For the proof, see Appendix A.5. □

The proof of the lemma shows that when its conditions are satisfied the bottom block matrix $U_n(l(i-1)+1{:}li, :)$ in U_n is zero. Therefore, when the matrix $(U_n|U_n^{\perp})$ is orthonormal, the bottom submatrix $U_n^{\perp}(l(i-1)+1{:}li, :)$ has to have full row rank. In this way, we have proved the assertion made after Theorem 4 of Part 1.

The above two lemmas in combination with Lemmas 1 and 2 lead to the main theorem of this section.

Theorem 1: *Let,*

(1) *the input* u_k *be such that condition* (28) *of Part 1 (or condition* (11) *of this Part), and the assumption in the basic identification problem hold;*

(2) *the perturbation to the output* v_k *be zero-mean white noise;*

(3) *the underlying deterministic plant* $\boldsymbol{P}$ *be representable by an FIR model* (1) *of order* κ *and a state space model given by* (1)–(2) *of Part 1 of order* n*;*

(4) *the dimension parameter* i *in the MOESP realization scheme satisfy:*

$$i > n \quad \textit{and} \quad i \geq \kappa \tag{14}$$

(5) *the Markov parameters* $[D \;\; CB \;\; \ldots \;\; CA^{i-2}B]$ *be exactly known:*

then the quadruple of system matrices $[\hat{A}_T, \hat{B}_T, \hat{C}_T, \hat{D}]$, *representing an* n*th order state-space model realized with the MOESP1 algorithm, is asymptotically unbiased.*

Proof: For the proof, see Appendix A.6. □

In the theorem, the order of the system was assumed to be given. However, identifying the matrices $\Gamma_i X_{1,N}$ and $V_{1,i,N}$ in the proof of Theorem 1 with the matrices F_N and V_N in Lemma 2, the latter Lemma demonstrates that the singular values in the SVD of $(\Gamma_i X_{1,N} + V_{1,i,N})$ will also reveal this quantity. This features requires the separation of the singular values of the matrix $(\Gamma_i X_{1,N} + V_{1,i,N})$ in those corresponding to the 'signal' or 'error-free' component and those corresponding to the 'noise' component. In practice, this might not be trivial at all.

2.4. *The MOESP2 algorithm*

The equation given at the end of the proof of Theorem 1 in Appendix A.6, i.e.

$$(A_T|B_T) = ((U_n^{(1)})\dagger U_n^{(2)}|(U_n^{(1)})\dagger(\Gamma_{i-1}B)) \tag{15}$$

shows that when the perturbations $v_k \equiv 0$ and the Markov parameters in the matrix H_i are exactly known, the solutions for the system matrices $(A_T|B_T)$ only require the column space of the matrix U_n (or Γ_i) in addition to the restricted set of Markov parameters $(\Gamma_{i-1}B)$. Furthermore, the additional and often cumbersome requirement $i \geq \kappa$, stated in (14), was only necessary to make use of (13) of Lemma 1. Therefore, the proof of Theorem 1 reveals that this condition does not intervene when directly computing estimates of the system matrices, as given by (15). Therefore, this would yield unbiased estimates without the constraint $i \geq \kappa$. A summary of this way of computing a realization for the case $v_k \equiv 0$ follows.

The elementary MOESP2 algorithm

Given:

(i) an estimate of the underlying system order n;

(ii) a dimension parameter i, satisfying:

$$i > n \tag{16}$$

(iii) the first i Markov parameters $h_s = CA^{s-1}B$ for $s = 1, \ldots, i-1$ and $h_0 = D$;

(vi) the input and output data sequences $[u_1, u_2, \ldots, u_{N+i-1}]$ and $[y_1, y_2, \ldots, y_{N+i-1}]$, with $N \gg mi$;

do the following.

Step 1. Construct the Hankel matrices $U_{1,i,N}$ and $Y_{1,i,N}$ and the lower triangular Toeplitz matrix H_i, all defined in (7) and (8) of Part 1.

Step 2. Achieve a data compression via te RQ factorization given in (25) of Part 1.

Step 3. Compute the SVD, of the matrix $[(R_{21} - H_iR_{11})|R_{22}]$, given as $U_nS_nV_n^T$.

Step 4. Compute the quadruple of system matrices $[A_T, B_T, C_T, D]$ by solving the following set of equations:

$$U_n^{(1)}A_T = U_n^{(2)} \tag{17}$$

$$U_n^{(1)}B_T = (\Gamma_{i-1}B) \tag{18}$$

and extract the following matrices:

$$C_T = \text{first } l \text{ rows of the matrix } U_n \tag{19}$$

$$D = \text{the (estimated) Markov parameter } h_0 \tag{20}$$

The main difference between the MOESP1 (see §§ 4.2–4.3 of Part 1) and the MOESP2 algorithm is that, in the latter the key part consists of approximating

the column space of the extended observability matrix Γ_i. As demonstrated in Theorem 3 of Verhaegen and Dewilde (1992), the key part of the MOESP1 algorithm is the approximation of the row space of the matrix $X_{1,N}$. In this way, the MOESP2 algorithm is strongly related to the classical realization scheme based on Markov parameters only, but also to the ordinary MOESP approach.

3. Comparison of the MOESP2 scheme with the classical realization scheme based on Markov parameters only

In the asymptotic analysis of the unbiasedness of the MOESP1 and MOESP2 algorithms in Theorem 1, we have assumed the exact knowledge of a restricted set of Markov parameters. Therefore, one may wonder why it is not sufficient to realize immediately a quadruple of system matrices from these Markov parameters only. The latter approach, as outlined in a system identification context in Kung (1978), is referred to in this paper as the classical approach. To answer this question, it is necessary to study the sensitivity of the computed results with respect to perturbations on the Markov parameters.

In this section, we study the effect of these errors on approximating the column space of the matrix Γ_i. For simplicity, we only treat the case where the input signal u_k is zero-mean white noise of unit variance ($\sigma_u \equiv 1$).

To distinguish between similar quantities that are approximated in both algorithms, the relevant ones related to the MOESP2 scheme are marked in **bold**.

3.1. *The classical SMI scheme*

The description of the classical algorithm in this paper is mainly based on the outline given in Kung (1978). A summary of the algorithm to compute the column space of the extended observability matrix is given next.

The CLASSIC algorithm

Given

(i) an estimate of the system order n;

(ii) the Markov parameters $h_s = CA^{s-1}B$ for $s = 1, \ldots, 2i-1$ for $i > n$ and $h_0 = D$;

do the following.

Step 1. Construct the Hankel matrix H_i^c:

$$H_i^c = \begin{bmatrix} h_1 & h_2 & \cdots & h_i \\ h_2 & h_3 & \cdots & h_{i+1} \\ \vdots & & & \vdots \\ h_i & & \cdots & h_{2i-1} \end{bmatrix} = \Gamma_i \Delta_i \tag{21}$$

with $\Delta_i = [B \; AB \; \ldots \; A^{i-1}B]$.

Step 2. Compute the SVD of the Hankel matrix H_i^c:

$$H_i^c = U_n S_n V_n^{\mathrm{T}} \tag{22}$$

with S_n an $n \times n$ diagonal matrix, $U_n \in \mathbb{R}^{l.i \times n}$ and $V_n \in \mathbb{R}^{m.i \times n}$.

Step 3. Identify the column space of H_i^c:

$$\text{span}_{\text{col}}(\Gamma_i) = U_n \tag{23}$$

The computation of a realization is done as described in Step 4 of the MOESP2 algorithm.

3.2. *Sensitivity analysis*

In Appendix B, we summarize two propositions discussing the perturbation of invariant subspaces of a symmetric matrix. These propositions will be used in the sensitivity analysis. In the beginning of this section, we also introduce the notation $\lambda(M)$ to denote the spectrum of the matrix M and $\|M\|_2$ to denote the 2-norm of a matrix M.

In this section we analyse the numerical sensitivity of calculating the column space of Γ_i (or $\boldsymbol{\Gamma}_i$) with respect to perturbations on the data. According to the algorithmic summaries of the MOESP2 algorithm (see Step 3 in § 2.4) and the CLASSIC algorithm (see Step 2–3 in § 3.1), such a basis is obtained via the singular value decomposition. Hence, we should study the effect of the errors on the computation of U_n (respectively $\boldsymbol{U}_n$). However, assuming that the effect of the estimation errors is of different orders of magnitude larger than errors made during the numerical computations it is subsequently valid to consider the influence of the estimation errors on the calculation of invariant subspaces in a symmetric eigenvalue problem.

3.2.1. *The perturbed symmetric eigenvalue problem related to the CLASSIC algorithm.* Let the estimated Markov parameters $\tilde{h}_j$ be perturbations of the true Markov parameters h_j, that is $\tilde{h}_j = h_j + \delta h_j$, for $j = 1, \ldots, 2i-1$, then the perturbation of the Hankel matrix H_i^c is denoted as:

$$\tilde{H}_i^c = H_i^c + \delta H_i^c \tag{24}$$

Hence,

$$\tilde{H}_i^c(\tilde{H}_i^c)^{\mathrm{T}} = H_i^c(H_i^c)^{\mathrm{T}} + H_i^c(\delta H_i^c)^{\mathrm{T}} + \delta H_i^c(H_i^c)^{\mathrm{T}} + \delta H_i^c(\delta H_i^c)^{\mathrm{T}} \tag{25}$$

Denote the eigenvalue decomposition of this matrix by:

$$\tilde{H}_i^c(\tilde{H}_i^c)^{\mathrm{T}} = [\tilde{U}_n | \tilde{U}_n^{\perp}] \left[\begin{array}{c|c} \tilde{S}_n^2 & 0 \\ \hline 0 & \star \end{array}\right] \left[\begin{array}{c} (\tilde{U}_n)^{\mathrm{T}} \\ \hline (\tilde{U}_n^{\perp})^{\mathrm{T}} \end{array}\right] \tag{26}$$

This matrix will, in general, have full rank. On the other hand, its unperturbed counterpart has rank $n < l.i$.

In view of Proposition 1 (See Appendix B), we now denote the unperturbed symmetric matrix and its perturbation respectively as:

$$M_C = H_i^c(H_i^c)^{\mathrm{T}} = \Gamma_i \Delta_i \Delta_i^{\mathrm{T}} \Gamma_i^{\mathrm{T}} \tag{27}$$

$$E_C = H_i^c(\delta H_i^c)^{\mathrm{T}} + \delta H_i^c(H_i^c)^{\mathrm{T}} + \delta H_i^c(\delta H_i^c)^{\mathrm{T}} \tag{28}$$

The dimension parameters q and r used in Proposition 1 (see Appendix B) are now equal to $l.i$ and n respectively. In the above two equations, the subscript C refers to the CLASSIC scheme.

3.2.2. *The perturbed symmetric eigenvalue problem related to the MOESP2 algorithm.* Assume, as before, that the estimated Markov parameters $\tilde{h}_j$ are perturbations of the true parameters h_j, that is $\tilde{h}_j = h_j + \delta h_j$, for $j = 1, \ldots, i$, then the perturbation of the Toeplitz matrix $\boldsymbol{H}_i$ in (8) of Part 1 is denoted as:

$$\tilde{\boldsymbol{H}}_i = \boldsymbol{H}_i + \delta \boldsymbol{H}_i \tag{29}$$

Hence, the perturbation of $\boldsymbol{\Gamma}_i X_{1,N}$ (due to the errors v_k and δh_j), denoted by $\widetilde{\boldsymbol{\Gamma}_i X_{1,N}}$ equals:

$$\widetilde{\boldsymbol{\Gamma}_i X_{1,N}} = Z_{1,i,N} - \tilde{\boldsymbol{H}}_i U_{1,i,N} = \boldsymbol{\Gamma}_i X_{1,N} - \delta \boldsymbol{H}_i U_{1,i,N} + V_{1,i,N} \tag{30}$$

Since, $\boldsymbol{v}_k$ and $\boldsymbol{u}_k$ are orthogonal and hence $\frac{1}{N} V_{1,i,N} U_{1,i,N}^{\mathrm{T}} = \varepsilon_N^4 E_N^4$ and since by Lemma 2 of Part 1, $\frac{1}{N} X_{1,N} U_{1,i,N}^{\mathrm{T}} = \varepsilon_N^3 E_N^3$, and making use of the expression for $X_{1,N}$ as given in (A 7) of Part 1 and the white noise property of $\boldsymbol{u}_k$ as expressed by (14) of Part 1, we find:

$$\frac{1}{N} \widetilde{\boldsymbol{\Gamma}_i X_{1,N}} (\widetilde{\boldsymbol{\Gamma}_i X_{1,N}})^{\mathrm{T}} = [\boldsymbol{\Gamma}_i [\Delta_i | \Delta_i^r] \begin{bmatrix} \Delta_i^{\mathrm{T}} \\ (\Delta_i^r)^{\mathrm{T}} \end{bmatrix} \boldsymbol{\Gamma}_i^{\mathrm{T}} + \delta \boldsymbol{H}_i \delta \boldsymbol{H}_i^{\mathrm{T}}] \sigma_u^2 + \sigma_v^2 I_{l.i} + \Delta \tag{31}$$

where $\Delta_i^r = A^i [B \;\; AB \;\; A^2 B \;\; \ldots]$ and Δ represents second-order effects such as $(1/N) V_{1,i,N} U_{1,i,N}^{\mathrm{T}} \delta \boldsymbol{H}_i^{\mathrm{T}}$ and other terms that vanish for $N \to \infty$.

Now we express the eigenvalue decomposition of the matrix product in (31) as:

$$\frac{1}{N} \widetilde{\boldsymbol{\Gamma}_i X_{1,N}} (\widetilde{\boldsymbol{\Gamma}_i X_{1,N}})^{\mathrm{T}} = [\tilde{\boldsymbol{U}}_n | \tilde{\boldsymbol{U}}_n^{\perp}] \left[\begin{array}{c|c} \tilde{\boldsymbol{S}}_n^2 & 0 \\ \hline 0 & \star \end{array}\right] \left[\begin{array}{c} (\tilde{\boldsymbol{U}}_n)^{\mathrm{T}} \\ \hline (\tilde{\boldsymbol{U}}_n^{\perp})^{\mathrm{T}} \end{array}\right] \tag{32}$$

Then, since $\sigma_u^2 \equiv 1$, we have the following pair of matrices characterizing the perturbed eigenvalue problem in Proposition 1 (see Appendix B):

$$M_{\mathrm{M}} = \boldsymbol{\Gamma}_i [\Delta_i | \Delta_i^r] \begin{bmatrix} \Delta_i^{\mathrm{T}} \\ (\Delta_i^r)^{\mathrm{T}} \end{bmatrix} \boldsymbol{\Gamma}_i^{\mathrm{T}} + \sigma_v^2 I_{l.i} \tag{33}$$

which clearly has full rank and which, according to Proposition 2 (see Appendix B), has the same invariant subspace as $M_{\mathrm{M}} - \sigma_v^2 I_{l.i}$, and,

$$E_{\mathrm{M}} = \delta \boldsymbol{H}_i \delta \boldsymbol{H}_i^{\mathrm{T}} + \Delta \tag{34}$$

The dimension parameters q and r of Proposition 1 (see Appendix B) again equal $l.i$ and n respectively. The subscript M is used to indicate correspondence with the elementary MOESP2 algorithm.

3.2.3. *Discussion.* Comparing the matrices M_{C} in (27) and M_{M} in (33) we conclude that:

$$M_{\mathrm{M}} - M_{\mathrm{C}} = \Gamma_i \Delta^r (\Delta^r)^{\mathrm{T}} \Gamma_i^{\mathrm{T}} + \sigma_v^2 I_{l.i}$$

which is clearly positive definite and hence $M_{\mathrm{M}} > M_{\mathrm{C}}$ or, the minimum eigenvalue ($\neq \sigma_v^2$) of M_{M} is larger than the minimum eigenvalue ($\neq 0$) of M_{C}. Denoting,

$$\delta_{\mathrm{M}} = \min_{\substack{\lambda_{\mathrm{M}} \in \lambda(M_{\mathrm{M}}) \\ \lambda_{\mathrm{M}} \neq \sigma_v^2}} |\lambda_{\mathrm{M}}| - \|E_{\mathrm{M},11}\|_2 - \|E_{\mathrm{M},22}\|_2 \tag{35}$$

and

$$\delta_C = \min_{\substack{\lambda_C \in \lambda(M_C) \\ \lambda_C \neq 0}} |\lambda_C| - \|E_{C,11}\|_2 - \|E_{C,22}\|_2 \tag{36}$$

and assuming (1) that $\delta_M > 0$, $\delta_C > 0$ and (2) $\delta_C < \delta_M$, then Proposition 1 (see Appendix B) asserts that the invariant subspace U_n of M_C is more sensitive to the additive errors considered than the same invariant subspace U_n of M_M.

Now, the assumption $\delta_C < \delta_M$ will generally be satisfied because of the significance of either terms in $M_M - M_C$ and assuming that all terms in the perturbations E_C and E_M are comparable. Similarly, the assumption $\delta_C > 0$ and $\delta_M > 0$ is generally true provided that the signal-to-noise ratio is large enough. When the latter conditions are violated, the invariant subspace of interest cannot be retrieved by the numerical scheme suffering from the violation.

A number of remarks are in order at this point.

(1) Since the difference $M_M - M_C$ equals

$$\Gamma_i A^i [\Delta_i | \Delta_i^r] \begin{bmatrix} \Delta_i^T \\ (\Delta_i^r)^T \end{bmatrix} (A^i)^T \Gamma_i^T + \sigma_v^2 I_{l.i}$$

we observe that its 2-norm is affected by the 2-norm of the matrix A^i. Therefore, when the underlying system has its poles inside the unit circle the superiority of the MOESP2 algorithm decreases by increasing i. Based on this observation, we conclude that the insensitivity of the MOESP2 algorithm compared with the CLASSIC algorithm will be significant when the system has its eigenvalues close to the unit circle and/or i is small compared with κ in (1) or as defined later in (41). Systems that can be characterized in this way will be labelled as 'marginally stable systems'. The presence of the noise term v_k demonstrates working out the advantage of the elementary MOESP2 algorithm.

(2) In the derivation of the symmetric eigenvalue problem in (31) related to the MOESP2 algorithm, we implicitly assumed the system to be operating from time instant $k = -\infty$ and on. When we start the data collection and excitation of the plant at a finite time (and at zero state), the eigenvalues of the matrix M_M decrease in magnitude. This technical detail increases the sensitivity of the MOESP2 algorithm. The effect on the CLASSIC algorithm will not be analysed.

(3) In the present outline of both identification approaches, nearly twice the number of Markov parameters are required in the CLASSIC algorithm. However, when using all available Markov parameters, as with the CLASSIC scheme, we see that the set of equations, (17), which determine $\hat{A}_T$ has more rows then is the case for a similar set of equations in the CLASSIC algorithm. Therefore, we can expect a better error averaging within the MOESP2 scheme.

To summarize, the main observation of the performed perturbation study in this section is that the column space of the extended observability matrix Γ_i is calculated more accurately with the MOESP2 algorithm. As a consequence, the results derived from this shift-invariant subspace will also be more accurate. In this sense, the MOESP2 algorithm is numerically more robust.

4. Dominant mode extraction

4.1. *Framework of analysis*

An important aspect of the low-order identified model is that it accurately represents the system in a certain frequency range. In the literature, this problem is generally referred to as the model reduction problem. Nevertheless, looking at it more broadly and including the phenomenon studied in § 2, namely the ability to extract the deterministic part of the model from noisy measurements, it should be considered as a specific operation mode of dominant mode extraction.

The model reduction capabilities of the novel realization scheme are analysed in this section. We will assume the observations to be error-free. This would be compatible with realistic circumstances where first, the full order deterministic model is identified and next the model is reduced. Of course, it is desired to have a scheme that identifies a compact model using error-affected measurements. The insights in this section will indicate under which circumstances this is indeed possible. Later, we will present an experimental verification of the practical validity of these insights (see § 5.3).

4.2. *Optimality of the elementary MOESP implementations in model reduction*

From the outline of the MOESP1 and MOESP2 algorithm (see § 4.3 of Part 1 and § 2.4 of this Part) it is clear that, in the actual computation of the state space system matrices, the singular values and right singular vectors of the computed SVD do not intervene. Nevertheless, as stated in the paragraph following Theorem 1, these singular values bear 'crucial' information about the model order. Also, in revealing the model reduction capabilities, they reappear as is demonstrated in the next theorem.

Theorem 2: *Let*

(1) *the input* u_k *be such that condition* (28) *is satisfied;*

(2) *the underlying deterministic plant* **P** *be representable by a state space model* (1)–(2) *of Part 1 of order* n_1 *and the FIR model of order* κ, *see* (1) *of Definition* 1 *of this Part;*

(3) *the dimension parameter* i *in the MOESP schemes satisfy the conditions:*

$$i > n_1 \quad \text{and} \quad i \geqslant \kappa$$

(4) *the SVD of* $\Gamma_i X_{1,N}$ *be:*

$$\Gamma_i X_{1,N} = U_{n_1} S_{n_1} \bar{V}_{n_1}^{\mathrm{T}} = (U_n | U_n^{\perp}) \begin{pmatrix} S_1 V_1^{\mathrm{T}} \\ S_2 V_2^{\mathrm{T}} \end{pmatrix} \tag{37}$$

with the diagonal matrices $S_1 \in \mathbb{R}^{n \times n}$ $S_2 \in \mathbb{R}^{(n_1-n)\times(n_1-n)}$ *and* $n_1 > n$.

(5) *the system matrices* $(A_T|B_T)$ *of the full order system realized with the MOESP algorithm be partitioned as:*

$$(A_T|B_T) = \begin{matrix} n \\ n_1-n \end{matrix} \left(\begin{array}{c|c|c} \overset{n}{A_T(1,1)} & \overset{n_1-n}{A_T(1,2)} & \overset{m}{B_T(1,1)} \\ \hline A_T(2,1) & A_T(2,2) & B_T(2,1) \end{array} \right)$$

(6) *the state sequence over the time interval* $k = 1, \ldots, N$ *of the reduced order system:*

$$\hat{x}^n_{k+1} = A_T(1,1)\hat{x}^n_k + B_T(1,1)u_k \tag{38}$$

be denoted as:

$$\hat{X}^n_{1,N} = [\hat{x}^n_1 \quad \hat{x}^n_2 \quad \ldots \quad \hat{x}^n_N]$$

then,

(1) *the matrix* $A_T(1,1)$ *satisfies* $\|A_T(1,1)\|_2 \leq 1$

(2) $$\|S_2\|_2 \leq \left\| \begin{pmatrix} S_1 V_1^{\mathrm{T}} \\ S_2 V_2^{\mathrm{T}} \end{pmatrix} - \begin{pmatrix} \hat{X}^n_{1,N} \\ 0 \end{pmatrix} \right\|_2 \leq (1+\alpha)\|S_2\|_2 \tag{39}$$

with $\alpha = \beta(1 - \|A_T(1,1)\|_2^{N-1})/(1 - \|A_T(1,1)\|_2)$, *for* β *a constant generally close to* 1.

Proof: For the proof, see Appendix A.7. □

The above theorem leads to the following corollary and remark.

Corollary 3: *When the conditions of the above theorem are satisfied, the output matrix* C_T *computed by the MOESP algorithms corresponds to a submatrix of an orthonormal matrix. Hence, using* (39),

$$\begin{aligned} \|Y_{1,1,N} - \hat{Y}_{1,1,N} &= \left\| C_T \left[\begin{pmatrix} S_1 V_1^{\mathrm{T}} \\ S_2 V_2^{\mathrm{T}} \end{pmatrix} - \begin{pmatrix} \hat{X}^n_{1,N} \\ 0 \end{pmatrix} \right] \right\| \\ &\leq \|C_T\| \cdot \left\| \left[\begin{pmatrix} S_1 V_1^{\mathrm{T}} \\ S_2 V_2^{\mathrm{T}} \end{pmatrix} - \begin{pmatrix} \hat{X}^n_{1,N} \\ 0 \end{pmatrix} \right] \right\| \\ &\leq (1+\alpha)\|S_2\| \end{aligned} \tag{40}$$

The above theorem and corollary allow verification of the optimality of the model reduction step for a particular value of i. We can compute $\|Y_{1,1,N} - \hat{Y}_{1,1,N}\|$ for a particular value of i. Depending on its difference with $\|S_2\|$, the model reduction can be judged on its optimality. When the value of κ is known and manageably finite, we can meet the conditions stated in the theorem and hence, using the MOESP2 algorithm once, the above test will highlight the deviation from optimality. However, experimental evidence has demonstrated that when κ is large (infinite) the elementary MOESP schemes must be executed repeatedly, starting with a small value of i and then increasing it. This should be repeated until the discrepancy between the quantities in (40) are as small as possible within a prescribed tolerance.

Remark 1: The proof of Theorem 2 (see (A 9)) also states that the calculation of the reduced-order model, defined by the system matrices $[A_T(1,1)|B_T(1,1)]$, only requires knowledge of the part U_n of the column space of Γ_i. The calculation of the other parts of A_T and B_T requires knowledge of $U_n^{\perp}$. Hence, we can interpret this splitting of the column space of the matrix Γ_i into matrices with orthogonal columns as an independent parametrization of the different parts in the model. In the framework of parametric system identification, set up in Ljung (1987), it is claimed that the independent parametrization of parts of the model used in a particular identification scheme, might lead to 'good' model

reduction capabilities. In the present framework, tne above theorem gives formal proof of this claim. □

The 'optimality' of the reduced-order state space model discussed in Theorem 2 can, in the case that the input is zero-mean white noise, be interpreted in terms of the Hankel singular values (Glover, 1984). This is indicated in our final theorem.

Theorem 3: *Let the conditions imposed in Theorem 2 be satisfied; let the input be zero-mean white noise with variance* $\sigma_u^2 = 1$, *satisfying condition* (14) *of Part 1, then the singular values in the matrices* S_1^2/N *and* S_2^2/N in (37) *asymptotically approach the Hankel singular values.*

Proof: For the proof, see Appendix A.8. □

5. Simulations

In this section, a number of experiments are reported to validate the insights obtained in the previous sections of this paper. These series of experiments can be subdivided into three parts. The first part verifies the asymptotic properties of the estimates obtained with the MOESP1 and MOESP2 algorithm. In the second part, an experimental comparison is performed between the CLASSIC and MOESP2 algorithms and the third part presents results demonstrating the model reduction capabilities of the elementary MOESP schemes.

All the numerical tests have been performed with the MATLAB package (Moler *et al.* 1987). When use is made of a white noise sequence in the tests, the internal random number generator of this package was used.

5.1. *Verification of the asymptotic unbiasedness of the elementary MOESP implementations*

In Theorem 1 (see condition (3)), the asymptotic unbiasedness of the MOESP1 algorithms required that the system to be identified has a FIR representation as given in (1). However, for a large class of linear time-invariant systems, the Markov parameters h_i only approach zero in the limit $i \to \infty$. Hence, in that case, condition (3) and condition (4) of Theorem 1 can never be satisfied. Nevertheless, it has been observed in similar simulation runs that the latter constraint can be relaxed somehow. When we define κ in condition (3) and (4) now as a function of some real parameter value τ.

$$\kappa(\tau) = \min_j \left\{ j : 1 > \frac{\sum_{l=0}^{j} \|h_l\|_2^2}{\sum_{l=0}^{\infty} \|h_l\|_2^2} =: \beta(j) \geq \tau \right\} \tag{41}$$

then the unbiasedness of the estimates obtained with the MOESP1 algorithm resulted in values of $\kappa(\tau)$ corresponding to values of τ close to 1·0.

The conflict between taking τ in (41) as close as possible to one and simultaneously limiting the dimension parameter value i in the MOESP1 algorithm becomes more pronounced when the underlying system has its eigenvalues close to the unit circle. The effect of this condition is analysed in the following experiment. Since the MOESP2 algorithm was claimed not to suffer

from this (over-)dimensioning, a comparison between both identification algorithms is performed.

5.1.1. *The mathematical model.* In this experiment the system to be identified is represented by a mathematical aircraft model, taken from Elliott (1977). This model describes the linearized longitudinal motion of an F-8 aircraft operating at 20 000 ft with an air speed of $V_0 = 620\,\text{ft}\,\text{s}^{-1}$ and an angle of attack $\alpha_0 = 0{\cdot}078\,\text{rad}$. The continuous state-space representation of the deterministic part of this motion due to deflections of the elevator angle δ_e is:

$$\frac{\mathrm{d}}{\mathrm{d}t}\begin{bmatrix} q \\ u \\ \alpha \\ \theta \end{bmatrix} = \begin{bmatrix} -0{\cdot}49 & 0{\cdot}00005 & -4{\cdot}8 & 0 \\ 0 & -0{\cdot}015 & -14{\cdot}0 & -32{\cdot}2 \\ 1{\cdot}0 & -0{\cdot}00019 & -0{\cdot}84 & 0 \\ 1{\cdot}0 & 0 & 0 & 0 \end{bmatrix}\begin{bmatrix} q \\ u \\ \alpha \\ \theta \end{bmatrix} + \begin{bmatrix} -8{\cdot}7 \\ -1{\cdot}1 \\ -0{\cdot}11 \\ 0 \end{bmatrix}\delta_e \tag{42}$$

where we refer to Elliott (1977) for an explanation of the other quantities beside δ_e. The second component of the state vector x is defined as the output quantity y_k. This output is perturbed by a zero-mean white noise sequence v_k with standard deviation equal to 0·5. The latter perturbation corresponds to a very high signal-to-noise ratio. The input sequence δ_e is also a zero-mean white noise sequence statistically independent from v_k and standard deviation 0·1. In the simulation, we used a discrete version of the continuous model. The discretization period and sampling period of input and output signals are equal to 0·05 s.

5.1.2. *Experiment 1.* We set up a Monte Carlo simulation study. In each run a different realization of the output z_k is generated for a fixed input sequence $\{\delta_e\}$. The length of each observation sequence is 1000 and a total of 25 runs was performed. The information flow through both algorithms considered is:

$$\{\delta_e(k)\},\ \{z_k\},\ h_0, \ldots, h_{39} \rightarrow \boxed{\text{MOESP } i = 40} \rightarrow \text{4th order model} \tag{43}$$

The eigenvalues are computed from the estimated system matrix $\hat{A}_T$ obtained in each run by both MOESP implementations. These estimated quantities are plotted in Fig. 2 on the left-hand side for the MOESP1 algorithm and on the right-hand side for the MOESP2 algorithm. The centres of the crosses in these figures correspond to the true eigenvalue locations.

5.1.3. *Discussion.* The results of the above experiment clearly show the effect described in Theorem 1. In addition, the MOESP2 implementation yields unbiased estimates for the conditions assumed in the experiment. These experimental conditions can be considered as critical, because the original system has eigenvalues very close to the unit circle, namely $0{\cdot}9997 \pm 0{\cdot}0038\text{j}$ (with $\text{j} = \sqrt{-1}$). Consequently, the integer κ defined in Theorem 1 or even as in the relaxed form given by (101), is of orders in magnitude larger than the order of the systems. Therefore, to make the MOESP1 algorithm compatible with the assumptions in Theorem 1, first of all, the computations burden drastically increases and second, the input has to be persistently excited of a very large order. This clearly demonstrates the advantages of the MOESP2 implementation. In additional experiments, however, it was observed that the MOESP1

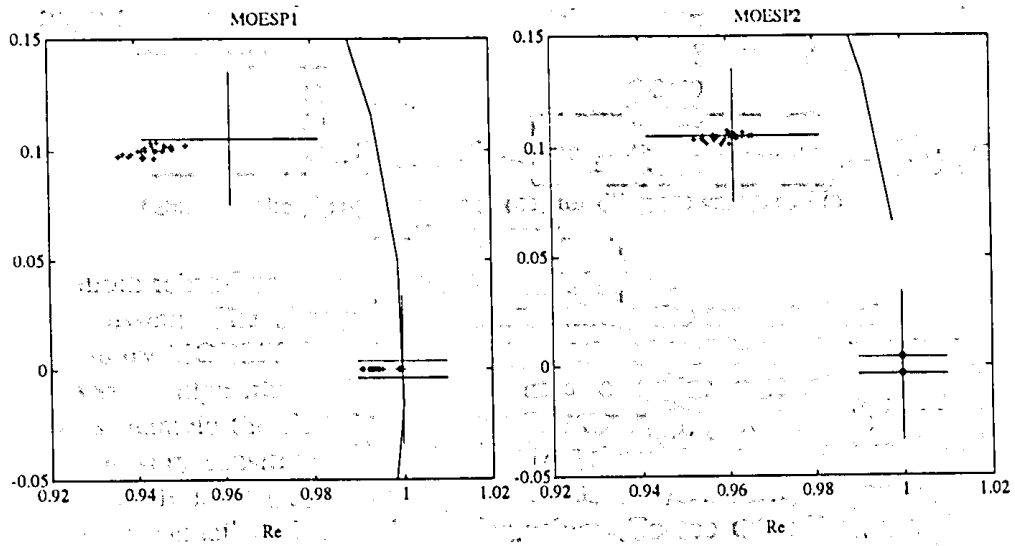

Figure 2. Poles of fourth order systems identified with the MOESP1 and 2 algorithms using batches of 1000 measurements.

algorithm has some degree of robustness with respect to violating conditions (3) and (4) of Theorem 1 for less 'critical' plants. In these experiments, the dimension parameter i in the MOESP1 algorithm could be taken at an order of magnitude smaller than $\kappa(\tau)$, defined in (41) for values of τ close to one, while still guaranteeing unbiased estimates.

5.2. *Comparing the CLASSIC and MOESP2 algorithm*

In the discussion following the analysis given in § 3, it was claimed that the MOESP2 algorithm will give more accurate results than the CLASSIC algorithm when only a restricted and perturbed set of Markov parameters are used in the calculations in both schemes.

The experimental conditions chosen to compare both schemes are in compliance with those assumed in the comparison study performed in § 3. Special attention will be given to the analysis of marginally stable systems.

5.2.1. *The mathematical model.* The mathematical model that represents the system to be identified is given by the following discrete state-space description:

$$x_{k+1} = \begin{bmatrix} 1{\cdot}92 & -0{\cdot}9316 \\ 1 & 0 \end{bmatrix} x_k + \begin{bmatrix} 1 \\ 0 \end{bmatrix} u_k \tag{44}$$

$$z_k = [0{\cdot}05 \quad 0{\cdot}025] x_k + v_k \tag{45}$$

The perturbation to the output v_k is a zero-mean white noise sequence with variance equal to 1·0. This corresponds to a relatively low signal-to-noise ratio. The input sequence u_k is also a zero-mean white noise sequence statistically independent from v_k with variance equal to 1·0.

5.2.2. *Experiment 2.* We set up a Monte Carlo simulation study. In each run, a different realization of the output sequence $\{z_k\}$ is generated while keeping the input sequence $\{u_k\}$ fixed. The length of the observations is restricted to 200.

The initial conditions are set equal to zero, corresponding to no past input. The information flow through the CLASSIC algorithm is:

$$\{u_k\},\ \{z_k\} \rightarrow \boxed{\text{Equation (2) } \kappa = 25} \rightarrow \tilde{h}_0, \ldots, \tilde{h}_{24}$$

$$\rightarrow \boxed{\text{CLASSIC } i = 12} \rightarrow \text{second-order model} \qquad (46)$$

The information flow through the MOESP2 algorithm is:

$$\{u_k\},\ \{z_k\} \rightarrow \boxed{\text{Equation (2) } \kappa = 25} \rightarrow \tilde{h}_0, \ldots, \tilde{h}_{11}$$

$$\rightarrow \boxed{\text{MOESP2 } i = 12} \rightarrow \text{second-order model} \qquad (47)$$

From the estimated system matrix $\hat{A}_T$ obtained in each run by both algorithms, we computed the eigenvalues. These estimates and their true values are plotted in Fig. 3 on the left-hand side of the CLASSIC algorithm and on the right-hand side for the MOESP2 algorithm.

A possible way to judge the choice of the dimension parameter i in both identification schemes is based on (41). For a fixed value of i, the amount of information present in the restricted number of Markov parameters considered by both schemes can be expressed by the value $\beta(i)$ defined in (41). In Table 1, we list this parameter for different values of the dimension parameter i used in the two schemes.

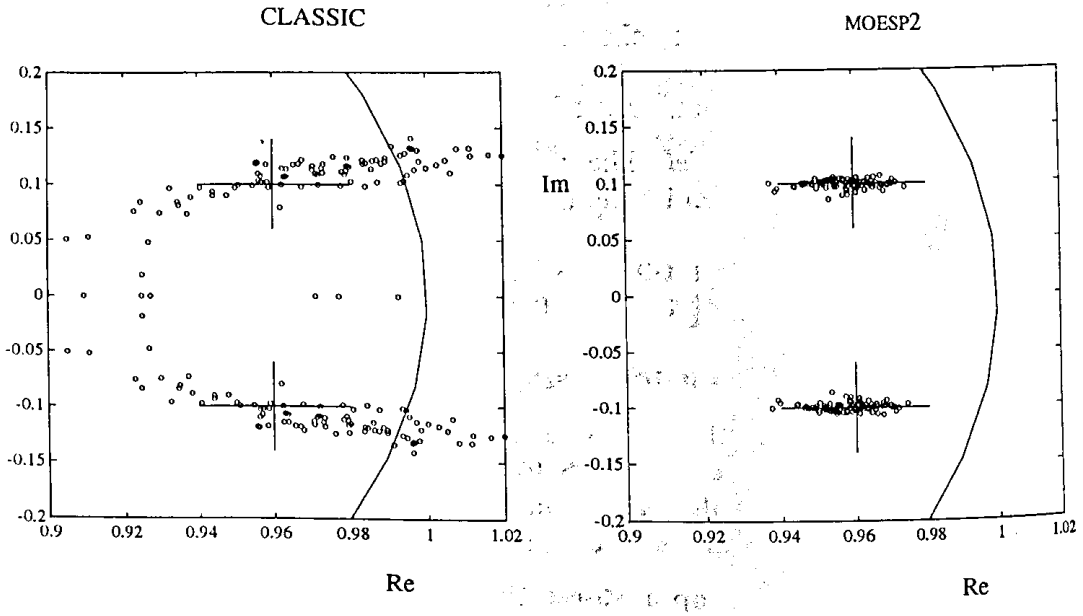

Figure 3. Poles of second order systems identified with the CLASSIC and MOESP2 algorithm using batches of 200 measurements.

Dimension parameter i	$\beta(i)$-parameter in (41)
12	0·3440
20	0·7580
24	0·8636

Table 1. The $\beta(i)$-parameter in (41) for different values of i in Experiment 2.

5.2.3. *Discussion.* The above experiment confirms the numerical robustness of the elementary MOESP2 implementation as outlined in § 3 and the sensitivity of the CLASSIC algorithm. Although it uses a major part of the Markov parameters, namely the first 24 corresponding to a $\beta(i)$ parameter in Table 1 of 0·8636, it is very sensitive to small errors on these parameters. Following the theoretical analysis of § 3, this numerical robustness/sensitivity depends on the separation of 'signal' and 'noise' singular values. To see this effect, we plotted the corresponding relevant singular values in Fig. 4. On the left-hand side, we plotted the singular values of $\widetilde{H}_i^c$ and on the right-hand side, we plotted the singular values of $(\widetilde{\Gamma_i X_{1,N}}/\sqrt{N})$ minus σ_v. The latter figure conveys the reasons outlined in § 3. Similar tests with larger batches of data, different dynamic systems, different signal-to-noise ratios, etc. showed a similar increased numerical robustness of the MOESP2 algorithm with respect to the class of errors considered. For the sake of brevity, we refrain from their presentation in this paper.

5.3. *Evaluating the model reduction capabilities of the elementary MOESP algorithm*

In Theorem 2 and Corollary 3, the model reduction capabilities of the MOESP algorithm were presented in terms of 2-norms of the errors on the state

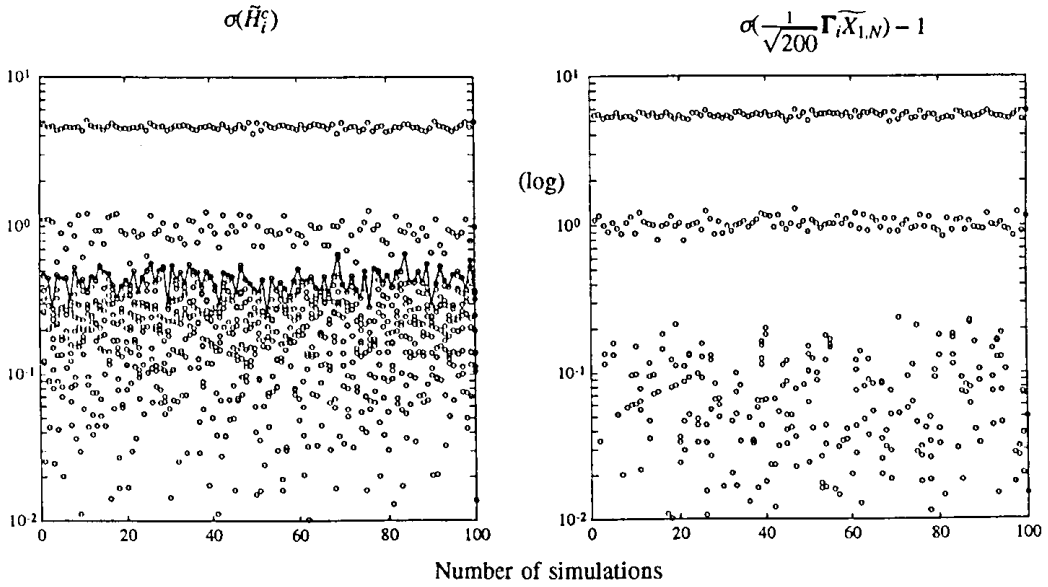

Figure 4. The relevant singular values to judge the numerical robustness of the CLASSIC and MOESP2 algorithm.

or output sequence reconstructed with the reduced order model. In this perspective, we may call a model reduction optimal if the values on both sides of the inequalities (39) and (40) are close to one another, i.e. when the constant α is in the vicinity of one.

A condition in the above theorem is again the constraint on the dimension parameter i as given by condition (3) of Theorem 2. In the experiment presented in this section, we study the robustness of the model reduction capabilities of MOESP with respect to violating this condition. Furthermore, we perform a comparison with the classical approximate model reduction approach based on a balanced realization, such as described by Moore (1981).

5.3.1. *The mathematical model.* The system considered in the next experiment is taken again from the aeronautical world. To demonstrate the MIMO capabilities of the MOESP approach, a mathematical model describing the longitudinal linearized motion of an F-4 aircraft at Mach 0·9 at an altitude of 15 000 ft is taken. The continuous state space description is:

$$\frac{\mathrm{d}}{\mathrm{d}t}x = \begin{bmatrix} -0{\cdot}0068 & 0{\cdot}0015 & -0{\cdot}6594 & 1 & 0 \\ 0{\cdot}0011 & -0{\cdot}494 & 14{\cdot}484 & -0{\cdot}0145 & 0 \\ 0{\cdot}341 & -1{\cdot}98 & -0{\cdot}488 & 0 & 0 \\ 0 & 0 & 1 & 0 & 0 \\ 0 & 0 & 0 & 0 & -1 \end{bmatrix} x + \begin{bmatrix} 0{\cdot}0321 & 0 \\ -0{\cdot}706 & 0 \\ -15{\cdot}99 & 0 \\ 0 & 0 \\ 0 & 0{\cdot}1 \end{bmatrix} u \tag{48}$$

$$y = \begin{bmatrix} 1{\cdot}022 & 0 & 0 & 0 & 0 \\ 0 & 0{\cdot}0689 & 0 & 0 & 0 \end{bmatrix} x \tag{49}$$

The different quantities in the state, input and output vector are not relevant in the present experiment and we refer to Elliott (1977) for an explanation of their physical meaning. The input vector consists of two independent zero-mean white noise sequences with variance equal to 1·0. The output sequences used in the model reduction are unperturbed. In the simulation study, the continuous model was discretized for a period of 0·05 s. The model reduction analysis is based on this discrete model.

5.3.2. *Experiment 3.* The model in (48)–(49) is used to generate a single batch of input and output samples with a length of 500. The MOESP2 algorithm uses this data along with the true and necessary Markov parameters to identify a state-space model of order $n = 3$. The true order n_1 of the underlying system is five. In a first part of this experiment, the dimension parameter i was set equal to 16. In a second part, this value was increased to 60. The results of this experiment are summarized in Table 2. The top three quantities in this table correspond to values defined in Theorem 2. The bottom quantity, namely the 2-norm of a part of the impulse response, allows one to quantify the violation of the constraint in condition (3) of Theorem 2.

Norm quantity	$i = 60$	$i = 16$	Balanced realization
$\left\|\begin{pmatrix} S_1 V_1^T \\ S_2 V_2^T \end{pmatrix} - \begin{pmatrix} \hat{X}_{1,N}^{n=3} \\ 0 \end{pmatrix}\right\|$	8·893	12·261	30·338
$\|Y_{1,1,N} - \hat{Y}_{1,1,N}\|$	2·178	2·952	47.035
$\|S_2\|$	2·052	0.3145	1.6841
$\sum_{l=0}^{i} \|h_l\|^2$	0·3486	0·1750	

Table 2. Values of the norm quantities specified in Theorem 2 to judge the optimality of the reduced third order model.

5.3.3. *Discussion.* The above experiment demonstrates the robustness of the MOESP2 algorithm in model reduction with respect to violating the constraint in condition (3) of Theorem 2. This observation can be made since for $i = 16$ or $i = 60$ only a minor part of the impulse response has been considered. This may be observed by comparing the bottom values in Table 2 with the value that would result when taking i in this table equal to 4000. In the latter case, $\sum_{l=0}^{4000} \|h_l\|^2$ equals 5·7678. Therefore, when $i = 60$, the value of $\beta(60)$, defined in (41), is approximately 0·0604 and when $i = 16$, $\beta(16) \approx 0{\cdot}0303$.

6. Conclusions

In the second part of this series of papers, the identification and model reduction performances of the elementary MOESP scheme of Verhaegen and Dewilde (1992) are analysed.

The common thread in the performances of the elementary MOESP scheme is the parameter i, referred to as the dimension parameter since it determines the sizes of the data matrices handled by the algorithm. When this dimension parameter has to be chosen larger than or equal to the number of non-zero Markov parameters, it harms the performances of the MOESP algorithm mainly in two ways: (1) the computational burden increases significantly, since, for example, the number of flops (1 flop = 1 multiplication + 1 addition) in the RQ factorization increases proportional to i^2 and; (2) the data requirements in terms of the length of the observations and persistency of excitation become more critical.

It is demonstrated that the asymptotic unbiasedness of the estimates obtained with the elementary MOESP scheme presented in Verhaegen and Dewilde (1992), referred to as the MOESP1 scheme, stipulates the above condition. This analysis only considers the output quantity to be perturbed by zero-mean white noise errors. The same analysis automatically leads to the derivation of a second implementation of the elementary MOESP scheme, namely MOESP2. This alternative implementation is not indexed by this constraint on the dimension parameter i. Hence, for the latter scheme the dimension parameter i only has to be chosen larger than the order of the underlying system. In this way, the MOESP2 algorithm fully exploits the algorithmic advantage of using only the lower triangular factor of the RQ factorization in the elementary and ordinary

MOESP schemes. The constraint on the dimension parameter i allows for a very efficient execution of the RQ factorization and hence of all subsequent algorithmic steps.

These appealing computational properties are combined with an increased robustness by the MOESP2 scheme with respect to errors on the used data. This is based on a comparison with the classical approach based on Markov parameters only. The errors on the output are zero-mean white-noise errors. This property becomes significant when the number of non-zero (or larger than a prescribed tolerance) Markov parameters is large.

For a more general case, when these errors are arbitrarily coloured, it is possible to make the elementary MOESP schemes the building block of an iterative version. This would then correspond to an approach pursued in classical parametric model identification as described by Ljung (1987) and Söderström and Stoica (1989). In these classical iterative identification schemes, the simple linear least-squares method plays a key role. The schemes and analysis presented in this paper might serve as the crucial part in the design and analysis of iterative versions of the MOESP approach. However, we mention that it is possible to incorporate instrumental variables in an efficient way in the MOESP algorithmic structures, see the third part of this series of papers (Verhaegen 1993 or Verhaegen 1991 a). This extension has been demonstrated to make the MOESP schemes applicable to realistic identification problems, where the input and output signals are corrupted by zero-mean errors or arbitrary colouring.

The above insights are validated in a simulation study. A number of the experiments performed in this study are reported in this paper.

In the analysis of the model reduction capabilities of the elementary MOESP schemes, the finite impulse response constraint reappears. In this case, a procedure is derived to judge the optimality of the calculated reduced-order model making use of error-free observations. The optimality corresponds to the 2-norm of the errors on the reconstructed state or output sequence being as close as possible to the 2-norm of the matrix containing the rejected singular values. In the experimental verification study of this result, we demonstrated that the dimension parameter i can be constrained to practical values and still guarantee a reduced-order model of high quality, for example, compared with the classical balanced realization approach described in Moore (1981).

Based on this last observation and the asymptotic unbiasedness of the MOESP2 algorithm for a dimension parameter i of practical value, we are led to the assertion that the MOESP2 implementation allows efficient identification of a compact and accurate state space model from 'perturbed' input–output data.

Appendix

Proofs of the Corollaries, Lemmas and Theorems of Part 2

A.1. **Proof of Lemma 2:** Since $\tilde{F}_N = F_N + V_N$ it follows that:

$$\tilde{F}_N \tilde{F}_N^{\mathrm{T}} = F_N F_N^{\mathrm{T}} + F_N V_N^{\mathrm{T}} + V_N F_N^{\mathrm{T}} + V_N V_N^{\mathrm{T}}$$

Taking the limit for $N \to \infty$ of both sides and making use of (3)–(5), yields:

$$\lim_{N\to\infty}\frac{1}{N}\tilde{F}_N\tilde{F}_N^{\mathrm{T}} = U_F S_F^2 U_F^{\mathrm{T}} + \sigma^2 I_{l.i} = (U_F|U_F^{\perp})\left[\begin{array}{c|c} S_F^2+\sigma^2 I_n & 0 \\ \hline 0 & \sigma^2 I_{l.i-n}\end{array}\right]\left[\begin{array}{c} U_F^{\mathrm{T}} \\ \hline (U_F^{\perp})^{\mathrm{T}}\end{array}\right] \quad \text{(A 1)}$$

and the result of the lemma is established. □

A.2. **Proof of Corollary 1:** Since the singular values of $\tilde{F}_N$ are defined as the eigenvalues of the matrix $\tilde{F}_N\tilde{F}_N^{\mathrm{T}}$, we have:

$$\lim_{N\to\infty}\frac{1}{N}\left[\begin{array}{c|c} S^2_{\tilde{F}_N}(1{:}n,\ 1{:}n) & 0 \\ \hline 0 & S^2_{\tilde{F}_N}(n+1{:}l.i,\ n+1{:}l.i)\end{array}\right] = \left[\begin{array}{c|c} S_F^2+\sigma^2 I_n & 0 \\ \hline 0 & \sigma^2 I_{l.i-n}\end{array}\right]$$

Hence, since the diagonal entries (eigenvalues) of the matrix $S_F^2+\sigma^2 I_n$ and $\sigma^2 I_{l.i-n}$ differ, their corresponding invariant subspaces are uniquely determined (Golub and Van Loan 1989). In terms of the computed left singular subspaces and the limit in (6) or (A 1), the corollary holds. □

A.3. **Proof of Corollary 2:** From the conditions stipulated in the corollary, we have that

$$0 = \lim_{N\to\infty}\frac{1}{N}(U_F^{\perp})^{\mathrm{T}}(F_N + V_N)U_N^{\mathrm{T}}$$

Substituting the SVD of $\tilde{F}_N$ given in (7) yields:

$$= \lim_{N\to\infty}\frac{1}{N}(U_F^{\perp})^{\mathrm{T}}U_{\tilde{F}_N}(:,\ 1{:}n)S_{\tilde{F}_N}(1{:}n,\ 1{:}n)(V_{\tilde{F}_N}(:,\ 1{:}n))^{\mathrm{T}}U_N^{\mathrm{T}}$$

$$+ \lim_{N\to\infty}\frac{1}{N}(U_F^{\perp})^{\mathrm{T}}U_{\tilde{F}_N}(:,n+1{:}li)S_{\tilde{F}_N}(n+1{:}li,n+1{:}li)(V_{\tilde{F}_N}(:,n+1{:}li))^{\mathrm{T}}U_N^{\mathrm{T}}$$

Making use of the limits in (8), we obtain:

$$= \lim_{N\to\infty}\frac{1}{N}(U_F^{\perp})^{\mathrm{T}}U_F M_{1_N}S_{\tilde{F}_N}(1{:}n,\ 1{:}n)(V_{\tilde{F}_N}(:,\ 1{:}n))^{\mathrm{T}}U_N^{\mathrm{T}}$$

$$+ \lim_{N\to\infty}\frac{1}{N}M_{2_N}S_{\tilde{F}_N}(n+1{:}li,\ n+1{:}li)(V_{\tilde{F}_N}(:,\ n+1{:}li))^{\mathrm{T}}U_N^{\mathrm{T}}$$

Since the limit $\lim_{N\to\infty}(1/N)\tilde{F}_N U_N^{\mathrm{T}}$ exists, the limit $\lim_{N\to\infty}(1/N)S_{\tilde{F}_N}(1{:}n,\ 1{:}n)(V_{\tilde{F}_N}(:,\ 1{:}n))^{\mathrm{T}}U_N^{\mathrm{T}}$ exists, and since $(U_F^{\perp})^{\mathrm{T}}U_F = 0$, (9) holds. □

A.4. **Proof of Lemma 3:** We have to prove that

$$\rho\left(\lim_{N\to\infty}\frac{1}{N}\left[\begin{array}{c} T_1X_{1,N}+T_2V_{1,i,N} \\ \hline U_{1,1,N}\end{array}\right][X_{1,N}^{\mathrm{T}}T_1^{\mathrm{T}}+V_{1,i,N}^{\mathrm{T}}T_2^{\mathrm{T}} \quad U_{1,1,N}^{\mathrm{T}}]\right) = n+m$$

or alternatively that the matrix,

$$\lim_{N\to\infty} \frac{1}{N}\begin{bmatrix} T_1 X_{1,N} + T_2 V_{1,i,N} \\ U_{1,1,N} \end{bmatrix} [X_{1,N}^{\mathrm{T}} T_1^{\mathrm{T}} + V_{1,i,N}^{\mathrm{T}} T_2^{\mathrm{T}} \quad U_{1,1,N}^{\mathrm{T}}]$$

is positive definite. With the expressions in (10) and using the orthogonality between v_j and u_k, x_k, the above matrix equals:

$$\left[\begin{array}{c|c} T_1 P_X T_1^{\mathrm{T}} + \sigma_v^2 T_2 T_2^{\mathrm{T}} & T_1 R_{XU_1} \\ \hline R_{XU_1}^{\mathrm{T}} T_1^{\mathrm{T}} & R_{U_1} \end{array}\right]$$

Since the signal

$$\begin{bmatrix} T_1 x_k \\ u_k \end{bmatrix}$$

is persistently excited (of order 1), the above matrix is the sum of a positive definite matrix and a positive semidefinite matrix and hence is clearly positive definite. □

A.5. **Proof of Lemma 4:** Since U_n and $U_n^{\perp}$ are orthonormal, we have that:

$$[(U_n^{(1)})^{\mathrm{T}}\ U_n(l.(i-1)+1{:}l.i, :)^{\mathrm{T}}]\begin{bmatrix} (U_n^{\perp})^{(1)} \\ U_n^{\perp}(l.(i-1)+1{:}l.i, :) \end{bmatrix} = 0$$

or,

$$(U_n^{(1)})^{\mathrm{T}}(U_n^{\perp})^{(1)} = -U_n(l.(i-1)+1{:}l.i, :)^{\mathrm{T}} U_n^{\perp}(l.(i-1)+1{:}l.i, :)$$

Now we show that $U_n(l.(i-1)+1{:}l.i, :) \equiv 0$. Based on conditions (2) and (3) of the lemma, see Theorem 3 of Part 1, $\Gamma_i X_{1,N}$ has a SVD given as:

$$\Gamma_i X_{1,N} = [U_n | U_n^{\perp}] \left[\begin{array}{c|c} S_n & 0 \\ \hline 0 & 0 \end{array}\right] \begin{bmatrix} \bar{V}_n^{\mathrm{T}} \\ \star \end{bmatrix} = U_n S_n \bar{V}_n^{\mathrm{T}}$$

Hence,

$$(U_n^{\mathrm{T}} \Gamma_i) X_{1,N} = S_n \bar{V}_n^{\mathrm{T}}$$

Denote the matrix product $U_n^{\mathrm{T}}\Gamma_i$ by T, then since $S_n \bar{V}_n^{\mathrm{T}}$ is of rank n and $X_{1,N} \in \mathbb{R}^{n\times N}$, the square $n \times n$ matrix T is invertible. Then, we can denote $\Gamma_i X_{1,N}$ as,

$$\Gamma_i X_{1,N} = \Gamma_i T^{-1} T X_{1,N} = U_n S_n \bar{V}_n^{\mathrm{T}}$$

Hence, since $S_n \bar{V}_n^{\mathrm{T}}$ has full row rank n, we deduce from the previous two equations that

$$\Gamma_i T^{-1} = U_n \tag{A2}$$

which is denoted explicitly as

$$\Gamma_i T^{-1} = \begin{bmatrix} CT^{-1} \\ (CT^{-1})(TAT^{-1}) \\ \vdots \\ (CT^{-1})(TA^{i-1}T^{-1}) \end{bmatrix} = \begin{bmatrix} C_T \\ C_T A_T \\ \vdots \\ C_T A_T^{i-1} \end{bmatrix} = U_n$$

Based on the constraint on the dimension parameter i and the FIR representation of the plant $\boldsymbol{P}$, we conclude:

$$\begin{bmatrix} C_T \\ C_T A_T \\ \vdots \\ C_T A_T^{n-1} \end{bmatrix} A_T^{i-1} [B \quad A_T B_T \ \ldots \ A_T^{n-1} \quad B_T] \equiv 0$$

and therefore $A_T^{i-1} \equiv 0$. Hence the last block-row of U_n equals zero and the proof is completed. □

A.6. **Proof of Theorem 1:** We will only give the proof for the calculated system matrices A_T and B_T, since the solution with respect to the matrices C_T and D is similar. The proof is based on the construction of the solution to the least-squares problem in (40) of Part 1. Since, the Markov parameters in the matrix H_i in (9) of Part 1 are assumed to be exactly known, the matrix $(\Gamma_i X_{1,N} + V_{1,i,N})$ in (9) of Part 1 equals $Z_{1,i,N} - H_i U_{1,i,N}$. Hence, we can denote the least-squares sub-problem to calculate $(A_T|B_T)$ by:

$$\min_{(A_T,B_T)} \left\| (\tilde{U}_{n_N}^{(1)})\dagger(\Gamma_{i-1}X_{2,N} + V_{2,i-1,N}) - [A_T|B_T] \right.$$
$$\left. \underbrace{\begin{bmatrix} (\tilde{U}_{n_N}^{(1)})\dagger(\Gamma_{i-1}X_{1,N} + V_{1,i-1,N}) \\ \hline U_{1,1,N} \end{bmatrix}}_{} \right\|_F$$

with the additional subscript $(\cdot)_{\bullet N}$ now to indicate the dependency of the quantity $(\cdot)_\bullet$ on N.

Now denote the SVD of the matrix $\Gamma_i X_{1,N} + V_{1,i,N}$ as

$$\Gamma_i X_{1,N} + V_{1,i,N} = [\tilde{U}_{n_N}|\tilde{U}_{n_N}^{\perp}] \left[\begin{array}{c|c} \tilde{S}_{1_N} & 0 \\ \hline 0 & \tilde{S}_{2_N} \end{array}\right] \left[\begin{array}{c} \tilde{V}_{1_N}^{\mathrm{T}} \\ \hline \tilde{V}_{2_N}^{\mathrm{T}} \end{array}\right] \tag{A 3}$$

Then, identifying $\Gamma_i X_{1,N}$ with the matrix F_N in Lemma 2 and $V_{1,i,N}$ with the matrix V_N, we may conclude according to (8) that:

$$\lim_{N\to\infty} \tilde{U}_{n_N} = \lim_{N\to\infty} U_n M_{1_N} \quad \text{and} \quad \lim_{N\to\infty} \tilde{U}_{n_N}^{\perp} = \lim_{N\to\infty} U_n^{\perp} M_{2_N} \tag{A 4}$$

With the same identification of matrices, Corollary 2, shows that

$$\lim_{N\to\infty} \frac{1}{N} M_{2_N} \tilde{S}_{2_N} \tilde{V}_{2_N}^{\mathrm{T}} U_{1,1,N}^{\mathrm{T}} = 0 \tag{A 5}$$

Since, in the error-free case, see Theorem 3 (2) of Part 1, the matrix $(U_n^{(1)})\dagger\Gamma_{i-1}$ is a square invertible matrix, and since $\lim_{N\to\infty}(\tilde{U}_{n_N}^{(1)})\dagger = \lim_{N\to\infty} M_{1_N}^{\mathrm{T}}(U_n^{(1)})\dagger$, see the right-hand side limit in (A 4), there exists a particular N_1 such that for

$N \geq N_1$ the matrix $(\tilde{U}^{(1)}_{n_N})\dagger\Gamma_{i-1}$ is a square invertible matrix. Hence, by Lemma 3, for a fixed $N \geq N_1$, the underbraced matrix in the above least-squares sub-problem has a right inverse.

With the SVD of the matrix $\Gamma_i X_{1,N} + V_{1,i,N}$ in (A 3), we have the following expressions:

$$\Gamma_{i-1}X_{1,N} + V_{1,i-1,N} = [\tilde{U}^{(1)}_{n_N}|(\tilde{U}^{\perp}_{n_N})^{(1)}]\left[\begin{array}{c|c} \tilde{S}_{1_N} & 0 \\ \hline 0 & \tilde{S}_{2_N} \end{array}\right]\left[\begin{array}{c} \tilde{V}^{\mathrm{T}}_{1_N} \\ \hline \tilde{V}^{\mathrm{T}}_{2_N} \end{array}\right] \tag{A 6}$$

and

$$\Gamma_{i-1}AX_{1,N} + V_{2,i-1,N} = [\tilde{U}^{(2)}_{n_N}|(\tilde{U}^{\perp}_{n_N})^{(2)}]\left[\begin{array}{c|c} \tilde{S}_{1_N} & 0 \\ \hline 0 & \tilde{S}_{2_N} \end{array}\right]\left[\begin{array}{c} \tilde{V}^{\mathrm{T}}_{1_N} \\ \hline \tilde{V}^{\mathrm{T}}_{2_N} \end{array}\right]$$

Since, $\Gamma_{i-1}X_{2,N} = \Gamma_{i-1}AX_{1,N} + (\Gamma_{i-1}B)U_{1,1,N}$, we have

$$\Gamma_{i-1}X_{2,N} + V_{2,i-1,N} = [\tilde{U}^{(2)}_{n_N}|(\tilde{U}^{\perp}_{n_N})^{(2)}|(\Gamma_{i-1}B)]\left[\begin{array}{c} \tilde{S}_{1_N}\tilde{V}^{\mathrm{T}}_{1_N} \\ \hline \tilde{S}_{2_N}\tilde{V}^{\mathrm{T}}_{2_N} \\ \hline U_{1,1,N} \end{array}\right] \tag{A 7}$$

With the expressions in (A 6) and (A 7) and the definition $(\tilde{U}^{(1)}_{n_N})\dagger(\tilde{U}^{\perp}_{n_N})^{(1)} =: \tilde{M}_{3_N}$, the solution to the least-squares sub-problem can be denoted as

$$(\hat{A}_{T_N}|\hat{B}_{T_N}) = (\tilde{U}^{(1)}_{n_N})\dagger(\tilde{U}^{(2)}_{n_N}|(\tilde{U}^{\perp}_{n_N})^{(2)}|(\Gamma_{i-1}B))$$

$$\frac{1}{N}\left[\begin{array}{c|c} \tilde{S}^2_{1_N} & \tilde{S}_{1_N}\tilde{V}^{\mathrm{T}}_{1_N}U^{\mathrm{T}}_{1,1,N} \\ \hline \tilde{S}^2_{2_N}\tilde{M}^{\mathrm{T}}_{3_N} & \tilde{S}_{2_N}\tilde{V}^{\mathrm{T}}_{2_N}U^{\mathrm{T}}_{1,1,N} \\ \hline U_{1,1,N}\tilde{V}_{1_N}\tilde{S}_{1_N} + U_{1,1,N}\tilde{V}_{2_N}\tilde{S}_{2_N}\tilde{M}^{\mathrm{T}}_{3_N} & U_{1,1,N}U^{\mathrm{T}}_{1,1,N} \end{array}\right]$$

$$\left(\frac{1}{N}\left[\begin{array}{c|c} \tilde{S}^2_{1_N} + \tilde{M}_{3_N}\tilde{S}^2_{2_N}\tilde{M}^{\mathrm{T}}_{3_N} & \tilde{S}_{1_N}\tilde{V}^{\mathrm{T}}_{1_N}U^{\mathrm{T}}_{1,1,N} + \tilde{M}_{3_N}\tilde{S}_{2_N}\tilde{V}^{\mathrm{T}}_{2_N}U^{\mathrm{T}}_{1,1,N} \\ \hline U_{1,1,N}\tilde{V}_{1_N}\tilde{S}_{1_N} + U_{1,1,N}\tilde{V}_{2_N}\tilde{S}_{2_N}\tilde{M}^{\mathrm{T}}_{3_N} & U_{1,1,N}U^{\mathrm{T}}_{1,1,N} \end{array}\right]\right)^{-1} \tag{A 8}$$

Using the limits in (A 4) we have

$$\lim_{N\to\infty}\tilde{M}_{3_N} = \lim_{N\to\infty}M^{\mathrm{T}}_{1_N}(U^{(1)}_n)\dagger(U^{\perp}_n)^{(1)}M_{2_N} = 0 \tag{A 9}$$

The latter relationship holds because M_{1_N} and M_{2_N} are orthonormal matrices for all N, see (8), and because of Lemma 4. This result, in combination with the limit in (A 5) reduces the expression in (A 8) in the limit $N \to \infty$ to:

$$\lim_{N\to\infty}(\hat{A}_{T_N}|\hat{B}_{T_N}) = \lim_{N1\to\infty}(M^{\mathrm{T}}_{1_N}(U^{(1)}_n)\dagger U^{(2)}_n M_{1_N}|M^{\mathrm{T}}_{1_N}(U^{(1)}_n)\dagger(\Gamma_{i-1}B))$$

Without the errors v_k, that is for $\tilde{S}_{2_\infty} \equiv 0$ and $\tilde{U}_n = U_n$, the solution to the least-squares sub-problem is equal to:

$$(A_T|B_T) = ((U_n^{(1)})\dagger U_n^{(2)}|(U_n^{(1)})\dagger(\Gamma_{i-1}B))$$

Comparing the last two expressions, completes the proof of the theorem. □

A.7. **Proof of Theorem 2:** We only have to prove the upper bound. The system matrices A_T and B_T of the full n_1th order system, which is determined by the MOESP algorithm, satisfy the following overdetermined set of equations:

$$(U_{n_1}^{(1)})\dagger[U_{n_1}^{(2)}|(\Gamma_{i-1}B)\begin{bmatrix}S_{n_1}\bar{V}_{n_1}^{\mathrm{T}} \\ \hline U_{1,1,N}\end{bmatrix} = [A_T|B_T]\begin{bmatrix}(U_{n_1}^{(1)})\dagger U_{n_1}^{(1)}S_{n_1}\bar{V}_{n_1}^{\mathrm{T}} \\ \hline U_{1,1,N}\end{bmatrix} \quad \text{(A 10)}$$

Since, the conditions of Lemma 4 are satisfied:

$$(U_{n_1}^{(1)})\dagger = (U_{n_1}^{(1)})^{\mathrm{T}} \quad \text{(A 11)}$$

Now partition the matrices $U_{n_1}^{(1)}$ and $U_{n_1}^{(2)}$ according to the partitioning of U_{n_1} in (37), then a combination of (A 10) and (A 11) yields

$$\left[\begin{array}{c|c|c} (U_n^{(1)})^{\mathrm{T}}U_n^{(2)} & (U_n^{(1)})^{\mathrm{T}}(U_n^{\perp})^{(2)} & (U_n^{(1)})^{\mathrm{T}}(\Gamma_{i-1}B) \\ \hline ((U_n^{\perp})^{(1)})^{\mathrm{T}}U_n^{(2)} & ((U_n^{\perp})^{(1)})^{\mathrm{T}}(U_n^{\perp})^{(2)} & ((U_n^{\perp})^{(1)})^{\mathrm{T}}(\Gamma_{i-1}B)\end{array}\right]\left[\begin{array}{c}S_1V_1^{\mathrm{T}} \\ \hline S_2V_2^{\mathrm{T}} \\ \hline U_{1,1,N}\end{array}\right] =$$

$$\left[\begin{array}{c|c|c} A_T(1,1) & A_T(1,2) & B_T(1,1) \\ \hline A_T(2,1) & A_T(2,2) & B_T(2,1)\end{array}\right]\left[\begin{array}{c}S_1V_1^{\mathrm{T}} \\ \hline S_2V_2^{\mathrm{T}} \\ \hline U_{1,1,N}\end{array}\right] \quad \text{(A 12)}$$

Define, $Tx_k = (x_T)_k$ with T the non-singular transformation matrix representing the matrix product $(U_{n_1}^{(1)})^{\mathrm{T}}\Gamma_{i-1}$, $(X_T)_{1,N}^{\mathrm{top}} = S_1V_1^{\mathrm{T}}$, $(X_T)_{1,N}^{\mathrm{bot}} = S_2V_2^{\mathrm{T}}$ and

$$(X_T)_{2,N}^{\mathrm{top}} = [(U_n^{(1)})^{\mathrm{T}}U_n^{(2)}|(U_n^{(1)})^{\mathrm{T}}(U_n^{\perp})^{(2)}|(U_n^{(1)})^{\mathrm{T}}(\Gamma_{i-1}B)]\left[\begin{array}{c}S_1V_1^{\mathrm{T}} \\ \hline S_2V_2^{\mathrm{T}} \\ \hline U_{1,1,N}\end{array}\right]$$

the first n rows of the above partitioned set of equations can be written as:

$$(X_T)_{2,N}^{\mathrm{top}} = A_T(1,1)(X_T)_{1,N}^{\mathrm{top}} + B_T(1,1)U_{1,1,N} + A_T(1,2)(X_T)_{1,N}^{\mathrm{bot}}$$

Hence, since the state $\hat{x}_k^n$ evolves according to (38) the error between both state sequences in $(X_T)_{1,N+1}^{\mathrm{top}}$ and in $\hat{X}_{1,N+1}^n$ satisfies:

$$(X_T)_{2,N}^{\mathrm{top}} - \hat{X}_{2,N}^n = A_T(1,1)[(X_T)_{1,N}^{\mathrm{top}} - \hat{X}_{1,N}^n] + A_T(1,2)(X_T)_{1,N}^{\mathrm{bot}}$$

Further we introduce the following notation:

$$(X_T)_{1,N}^{\mathrm{bot}} = [w_1 \quad w_2 \quad \dots \quad w_N]$$

$$(X_T)_{1,N}^{\mathrm{top}} - \hat{X}_{1,N}^n = \tilde{X}_{1,N}^n = [\tilde{x}_1 \quad \tilde{x}_2 \quad \dots \quad \tilde{x}_N]$$

Then

$$[\tilde{x}_1 \quad \tilde{x}_2 \quad \dots \quad \tilde{x}_N] =$$

$$[0 \quad I \quad A_T(1,1) \quad \dots \quad A_T(1,1)^{N-2}]\,\mathrm{diag}\,(A_T(1,2))\begin{bmatrix} w_1 & w_2 & \dots & w_N \\ 0 & w_1 & \dots & w_{N-1} \\ \vdots & 0 & & \vdots \\ 0 & 0 & \dots & w_1 \end{bmatrix}$$

with $\mathrm{diag}\,(A_T(1,2))$ a block diagonal matrix $\in \mathbb{R}^{nN\times(n_1-n)N}$ with $A_T(1,2)$ on its diagonal. Therefore,

$$\|\tilde{X}^n_{1,N}\| \leq$$

$$\|[I \quad A_T(1,1) \quad \dots \quad A_T(1,1)^{N-2}]\| \cdot \|(A_T(1,2))\| \cdot \left\|\begin{bmatrix} w_1 & w_2 & \dots & w_N \\ 0 & w_1 & \dots & w_{N-1} \\ \vdots & 0 & & \vdots \\ 0 & 0 & \dots & w_1 \end{bmatrix}\right\|$$

Now we explicitly evaluate the norm quantities on the right-hand side of this inequality. Since $U_n^{(1)}$ and $(U_n^{\perp})^{(1)}$ are submatrices of orthonormal matrices,

$$\|A_T(1,2)\| = \|(U_n^{(1)})^{\mathrm{T}}(U_n^{\perp})^{(2)}\| \leq \|(U_n^{\perp})^{(2)}\| \leq 1$$

Also, since $A_T(1,1) = (U_n^{(1)})^{\mathrm{T}}U_n^{(2)}$, $\|A_T(1,1)\| \leq 1$, hence the eigenvalues of $A_T(1,1)$ are all within or on the unit circle. This proves the first part of the theorem. Hence, we have:

$$\|[I \quad A_T(1,1) \quad \dots \quad A_T(1,1)^{N-2}]\| \leq \sum_{j=0}^{N-2} \|A_T(1,1)\|_2^j = \frac{1-\|A_T(1,1)\|_2^{N-1}}{1-\|A_T(1,1)\|_2}$$

Since, $(X_T)^{\mathrm{bot}}_{1,N} = [w_1 \quad w_2 \quad \dots \quad w_N] = S_2V_2^{\mathrm{T}}$, we have for some constant β close to 1,

$$\left\|\begin{bmatrix} w_1 & w_2 & \dots & w_N \\ 0 & w_1 & \dots & w_{N-1} \\ \vdots & 0 & & \vdots \\ 0 & 0 & \dots & w_1 \end{bmatrix}\right\| \leq \beta\|S_2\|$$

From the above bounds, we conclude that

$$\|\tilde{X}^n_{1,N}\| \leq \alpha\|S_2\|$$

Hence,

$$\left\|\begin{bmatrix} S_1V_1^{\mathrm{T}} \\ S_2V_2^{\mathrm{T}} \end{bmatrix} - \begin{bmatrix} \hat{X}^n_{1,N} \\ 0 \end{bmatrix}\right\| \leq \left\|\begin{bmatrix} S_1V_1^{\mathrm{T}} \\ S_2V_2^{\mathrm{T}} \end{bmatrix} - \begin{bmatrix} (X_T)^{\mathrm{top}}_{1,N} \\ 0 \end{bmatrix}\right\| + \|(X_T)^{\mathrm{top}}_{1,N} - \hat{X}^n_{1,N}\|$$

$$\leq \|S_2\| + \alpha\|S_2\| \tag{A 13}$$

and the proof is completed.

A.8. **Proof of Theorem 3:** Recall from, for example, Glover (1984), that the Hankel singular values are the singular values of the matrix product of the

observability gramian $\mathcal{O}$ times the controllability gramian $\mathcal{C}$. Therefore, we now explicitly compute both gramians for the full order state-space model realized in the elementary MOESP schemes.

From (A 2), the observability gramian $\mathcal{O}$ equals:

$$\mathcal{O} = T^{-T}\Gamma_i^T\Gamma_i T^{-1} = U_n^T U_n = I$$

Making use of the representation by the MOESP algorithm of $(X_T)_{1,N} = (TX_{1,N})$ as

$$\left[\frac{S_{1_N}V_{1_N}^T}{S_{2_N}V_{2_N}^T}\right]$$

see Theorem 2 we can denote:

$$\frac{1}{N}TX_{1,N}X_{1,N}^T T^T = \frac{1}{N}\left[\begin{array}{c|c} S_{1_N}^2 & 0 \\ \hline 0 & S_{2_N}^2 \end{array}\right]$$

Substituting the expression in (52) from Part 1 for $(X_T)_{1,N}$ into the left-hand side of the above relationship; this expression is also equal to

$$= [B_T \quad A_T B_T \quad \dots \quad A_T^{\kappa-2}B_T]\frac{1}{N}$$

$$\begin{bmatrix} u_0 & u_1 & \dots & u_{N-2} \\ u_{-1} & & \dots & u_{N-2} \\ \vdots & & \dots & \\ u_{-\kappa+2} & & \dots & \end{bmatrix}\begin{bmatrix} u_0 & u_{-1} & \dots & u_{-\kappa+2} \\ u_1 & u_0 & & \\ \vdots & & & \vdots \\ u_{N-1} & u_{N-2} & & \end{bmatrix}\begin{bmatrix} B_T^T \\ B_T^T A_T^T \\ \vdots \\ B_T^T(A_T^{\kappa-2})^T \end{bmatrix}$$

Taking the limit of the right-hand side of the above equalities and making use of the white noise property in (14) of Part 1 yields

$$\lim_{N\to\infty}\frac{1}{N}\left[\begin{array}{c|c} S_{1_N}^2 & 0 \\ \hline 0 & S_{2_N}^2 \end{array}\right] = [B_T \quad A_T B_T \quad \dots \quad A_T^{\kappa-2}B_T]I_{m(\kappa-1)}\begin{bmatrix} B_T^T \\ B_T^T A_T^T \\ \vdots \\ B_T^T(A_T^{\kappa-2})^T \end{bmatrix} = \mathcal{C}$$

Hence, multiplication of the above expression for $\mathcal{O}$ and $\mathcal{C}$ leads to the desired result. □

Appendix B

Propositions

B.1. **Proposition 1:** (Taken from Golub and Van Loan (1989), p. 413). *Let M and $M + E$ be $q \times q$ symmetric matrices and let,*

$$Q = \underset{r}{q}[\underset{r}{Q_1} \quad \underset{q-r}{Q_2}]$$

with $r \leq q$, an orthogonal matrix such that the column range of Q_1 is an invariant subspace for M, that is $MQ_1 \subset Q_1$. Partition the matrices $Q^T MQ$ and $Q^T EQ$ as follows:

$$Q^{\mathrm{T}}MQ = \begin{bmatrix} M_{11} & 0 \\ 0 & M_{22} \end{bmatrix} \begin{matrix} r \\ q-r \end{matrix} \qquad Q^{\mathrm{T}}EQ = \begin{bmatrix} E_{11} & E_{12} \\ E_{21} & E_{22} \end{bmatrix} \begin{matrix} r \\ q-r \end{matrix}$$

$$\begin{matrix} r & q-r \end{matrix} \qquad \begin{matrix} r & q-r \end{matrix}$$

If

$$\delta = \min_{\substack{\lambda \in \lambda(M_{11}) \\ \mu \in \lambda(M_{22})}} |\lambda - \mu| - \|E_{11}\|_2 - \|E_{22}\|_2 > 0 \quad \text{and} \quad \|E_{12}\|_2 \leqslant \frac{\delta}{2}$$

then there exists a matrix $P \in \mathbb{R}^{(q-r)\times r}$ *satisfying,* $\|P\|_2 \leqslant (2/\delta)\|E_{21}\|_2$ *such that the columns of* $\tilde{Q}_1 = (Q_1 + Q_2P)(I + P^{\mathrm{T}}P)^{-1/2}$ *form an orthonormal basis of a subspace that is invariant for* $M + E$.

Proof: For the proof, see Steward (1973). □

B.2. **Proposition 2:** *Let* M *be a* $q \times q$ *symmetric matrix and let the column range of* Q_1, *with* $Q_1 \in \mathbb{R}^{q\times r}$ $(r < q)$, *be an invariant subspace of* M, *then* Q_1 *is an invariant subspace of* $M + \sigma^2 I$, *for any real number* σ.

Proof: Q_1 is an invariant subspace of $M + \sigma^2 I$, if, $(M + \sigma^2 I)Q_1 \subset Q_1$. This holds because $MQ_1 \subset Q_1$. □

Acknowledgment

The research of Dr Michel Verhaegen has been made possible by a fellowship from the Royal Dutch Academy of Arts and Sciences. The authors also thank the anonymous referees for their constructive and helpful comments that improved the readability of Parts 1 and 2 of this paper.

References

Chen, C. T., 1970, *Introduction to Linear System Theory*. (New York: Holt, Rinehart and Winston).

Elliott, J. R., 1977, NASA's Advanced Control law program for the F-8 digital fly-by-wire aircraft. *I.E.E.E. Transactions on Automatic Control*, **22**, 753–757.

Glover, K., 1984, All optimal Hankel-norm approximations of linear multivariable systems and their L_∞-error bounds, *International Journal of Control*, **39**, 1115–1193.

Golub, G., and Van Loan, C., 1989, *Matrix Computations* (Baltimore: Johns Hopkins University Press).

Ho, B. L., and Kalman, R. E., 1966, Effective construction of linear, state-variable models from input/output funtions. *Regelungstechnik*, **14**, 545–548.

Kung, S. Y., 1978, A new identification and model reduction algorithm via singular value decomposition. *Proceedings of the 12th Asilomar Conference on Circuits, Systems and Computers*, pp. 705–714.

Ljung, L., 1987, *System Identification: Theory for the User* (Englewood Cliffs, NJ: Prentice Hall).

Moler, C., Little, J., and Bangert, S., 1987, *PRO-MATLAB User's Guide*, The Math-Works Inc.

Moonen, M. and Vandewalle, J., 1990, QSVD approach to on- and off-line state space identification. *International Journal of Control*, **50**, 1133–1146.

Moore, B. C., 1981, Principal component analysis in linear systems: controllability, observability and model reduction. *I.E.E.E. Transactions on Automatic Control*, **26**, 17–32.

Söderström, T., and Stoica, P., 1989, *System Identification* (Englewood Cliffs, NJ: Prentice Hall).

Stewart, G. W., 1973, Error and perturbation bounds for subspaces associated with certain eigenvalue problems. *SIAM review*, **15**, 727–764.

VERHAEGEN, M., and DEWILDE, P., 1992, Subspace model identification. Part 1: The output-error state space model identification class of algorithms. *International Journal of Control*, **56**, 1211–1241.

VERHAEGEN, M., 1991 a, A novel non-iterative MIMO state space model identification technique. *Preprints of the 9th IFAC/IFORS symposium on Identification and System parameter estimation*, pp. 1453–1458; 1991 b, Robustness of the novel MOESP realization scheme. *Presented at the International Symposium on the Mathematical Theory of Networks and Systems*; 1993, Subspace model identification, Part 3: Analysis of the ordinary output-error state space model identification algorithm. *International Journal of Control*, **57**, to be published.